Clinical Cancer Research

Contribution of Adrenal Glands to Intratumor Androgens and Growth of Castration-Resistant Prostate Cancer

Elahe A. Mostaghel[1,2], Ailin Zhang[2], Susana Hernandez[2], Brett T. Marck[1], Xiaotun Zhang[3], Daniel Tamae[4], Heather E. Biehl[2], Maria Tretiakova[5], Jon Bartlett[2], John Burns[2], Ruth Dumpit[2], Lisa Ang[2], Alvin M. Matsumoto[1], Trevor M. Penning[4], Steven P. Balk[6], Colm Morrissey[3], Eva Corey[3], Lawrence D. True[5], and Peter S. Nelson[2]

Abstract

Purpose: Tumor androgens in castration-resistant prostate cancer (CRPC) reflect *de novo* intratumoral synthesis or adrenal androgens. We used C.B.-17 SCID mice in which we observed adrenal CYP17A activity to isolate the impact of adrenal steroids on CRPC tumors *in vivo*.

Experimental Design: We evaluated tumor growth and androgens in LuCaP35CR and LuCaP96CR xenografts in response to adrenalectomy (ADX). We assessed protein expression of key steroidogenic enzymes in 185 CRPC metastases from 42 patients.

Results: Adrenal glands of intact and castrated mice expressed CYP17A. Serum DHEA, androstenedione (AED), and testosterone (T) in castrated mice became undetectable after ADX (all $P < 0.05$). ADX prolonged median survival (days) in both CRPC models (33 vs. 179; 25 vs. 301) and suppressed tumor steroids versus castration alone (T 0.64 pg/mg vs. 0.03 pg/mg; DHT 2.3 pg/mg vs. 0.23 pg/mg; and T 0.81 pg/mg vs. 0.03 pg/mg, DHT 1.3 pg/mg vs. 0.04 pg/mg; all $P \leq 0.001$). A subset of tumors recurred with increased steroid levels, and/or induction of androgen receptor (AR), truncated AR variants, and glucocorticoid receptor (GR). Metastases from 19 of 35 patients with AR positive tumors concurrently expressed enzymes for adrenal androgen utilization and nine expressed enzymes for *de novo* steroidogenesis (HSD3B1, CYP17A, AKR1C3, and HSD17B3).

Conclusions: Mice are appropriate for evaluating adrenal impact of steroidogenesis inhibitors. A subset of ADX-resistant CRPC tumors demonstrate *de novo* androgen synthesis. Tumor growth and androgens were suppressed more strongly by surgical ADX than prior studies using abiraterone, suggesting reduction in adrenally-derived androgens beyond that achieved by abiraterone may have clinical benefit. Proof-of-concept studies with agents capable of achieving true "non-surgical ADX" are warranted.

Introduction

Androgen deprivation therapy (ADT) remains front-line treatment for patients with locally recurrent or metastatic prostate cancer, but patients uniformly progress to castration-resistant prostate cancer (CRPC). Residual intratumoral androgen are believed to play a critical role in maintaining ligand-dependent mechanisms of androgen receptor (AR) activation (1). The source of residual tissue androgens in castrated patients is believed to reflect the tumoral uptake and intracellular conversion of the adrenal androgens such as DHEA-sulfate (DHEAS) to testosterone (T) and dihydrotestosterone (DHT), and/or the *de novo* intratumoral synthesis of androgens from cholesterol or progesterone precursors (2, 3). CYP17A, expressed in the human adrenal gland, testis and ovary, is a single enzyme with one active site that catalyzes sequential but independent hydroxylase and lyase reactions both of which are required for converting pregnenolone or progesterone to the adrenal androgens DHEA or androstenedione (AED), respectively. In particular, circulating levels of DHEA-S (the primary circulating form of DHEA) in eugonadal men are extremely high and are not reduced by standard castration (CX) therapy (4–6).

The contribution of adrenal steroids to CRPC progression is directly supported by historical case reports documenting clinical responses to adrenalectomy (ADX) in men with CRPC (7), and indirectly supported in the modern era by the efficacy of the CYP17A inhibitor abiraterone (ABI) in decreasing circulating adrenal androgens and improving overall survival for men with metastatic prostate cancer in the androgen sensitive and CRPC settings (8, 9). A direct impact of adrenal CYP17A inhibition on suppressing prostate tissue androgens can be inferred from the decrease in prostate androgen levels achieved by addition of ABI to standard ADT in the neoadjuvant setting, wherein tumoral CYP17A expression and *de novo* intratumoral androgen synthesis

[1]Geriatric Research, Education and Clinical Center, VA Puget Sound Health Care System, Seattle, Washington. [2]Fred Hutchinson Cancer Research Center, Seattle, Washington. [3]Department of Urology, University of Washington, Seattle, Washington. [4]Perelman School of Medicine, University of Pennsylvania, Philadelphia, Pennsylvania. [5]Department of Pathology, University of Washington, Seattle, Washington. [6]Beth Israel Deaconess Medical Center, Boston, Massachusetts.

Note: Supplementary data for this article are available at Clinical Cancer Research Online (http://clincancerres.aacrjournals.org/).

Prior presentation: The results were presented in part at the American Society of Clinical Oncology Genito-Urinary Cancers Meeting, February 16–18, 2017, Orlando, FL (Abstract #224).

Corresponding Author: Elahe A. Mostaghel, VA Puget Sound Health Care System, 1100 Fairview Ave. N., P.O. Box 19024, Seattle, WA 98109. Phone: 206-667-1657; Fax: 206-667-2917; E-mail: emostagh@fredhutch.org

doi: 10.1158/1078-0432.CCR-18-1431

Translational Relevance

Response to the adrenal CYP17A inhibitor abiraterone in men with castration-resistant prostate cancer (CRPC) does not isolate the contribution of adrenally-derived steroids, as inhibition of intratumoral CYP17A and/or direct anti-AR effects cannot be excluded. We show C.B-17 SCID mice have adrenal CYP17A and are appropriate for testing inhibitors of adrenal steroidogenesis. Adrenalectomy suppressed tumor growth and androgens in two xenograft models of CRPC, and did so more strongly than prior studies using abiraterone. This suggests that reduction in adrenally-derived androgens beyond that achieved by abiraterone may have clinical benefit, and that proof of concept studies with agents that block ligand synthesis upstream of CYP17A, such as novel CYP11A inhibitors, are warranted. A subset of adrenalectomy-resistant tumors demonstrate *de novo* androgen synthesis and/or induction of AR, truncated AR variants, and GR, suggesting co-targeting AR or GR with abrogation of ligand synthesis will still be required for optimal clinical activity.

has not yet been upregulated (4, 10, 11). However, the antitumor activity of ABI in the setting of CRPC may also occur at the level of the tumor via inhibition of intratumoral CYP17A activity or via the direct anti-AR activity of ABI (2, 3, 12). Thus, the antitumor activity of ABI cannot necessarily be ascribed to inhibition of adrenal androgen synthesis alone, and the specific contribution of adrenally-derived steroids to intratumoral androgens and CRPC progression remains unproven.

The role of adrenal steroids in xenograft models of CRPC grown in castrated mice has not been previously investigated due to early literature suggesting a lack of functional CYP17A in rodent adrenal glands (13–17). Accordingly, the source of tumor androgens detected in patient-derived xenograft (PDX) models of CRPC grown in castrated male mice has been attributed solely to *de novo* intratumoral androgen synthesis (18). However, both historical studies using radioimmunoassays (RIA) and more recent studies using mass spectrometry (MS) have suggested functional adrenal CYP17A activity in rats and mice, including residual prostate androgens in castrated rats that were eliminated by ADX (19–23). Although the physiologic contribution of these steroid levels to normal prostatic biology was considered negligible (22, 23), this does not rule out a potential pathologic role in stimulating prostate tumor cells that are hypersensitive to androgen stimulation. We sought to experimentally demonstrate the contribution of adrenal steroids to intratumoral androgens and tumor progression in PDX models of CRPC grown in castrated male C.B-17 SCID mice in which we demonstrate adrenal CYP17A expression and activity.

Materials and Methods

Generation of Murine Samples from Intact, Castrated, and Adrenalectomized Mice

All experiments involving animals were performed in accordance with protocols approved by the Fred Hutchinson Center Institutional Animal Care Use Committee (file 1775) and recommendations in the Guide for the Care and Use of Laboratory Animals of the National Institutes of Health. All surgery was carried out under isofluorane anesthesia. All studies utilized male C.B-17 SCID mice (Taconic). Serum samples were collected by retro-orbital bleed from non-tumor bearing 18- to 20-week-old intact (eugonadal) male mice, an age-matched cohort of mice at 12 weeks after CX (CX performed at 6–8 weeks), and an age-matched cohort at 12 weeks after both CX and ADX. Serum was obtained from a separate cohort of intact and castrated male mice for independent measurement of serum steroids in the laboratory of Dr. Penning. Adrenal glands, kidney, liver, and quadriceps muscle were resected for tissue steroid measurements. Drinking water was replaced with normal saline supplemented with corticosterone (Sigma; 25 μg/mL in 0.2% ethanol–0.5% NaCl) at time of ADX (24). Adrenal glands for assessment of CYP17A methylation and transcript profiling were resected from intact and castrated male mice ranging in age from 12 to 36 weeks (3–8 months) to mirror the ages spanning the course of a typical xenograft study.

LuCaP Human Prostate Cancer PDX Models and CRPC Tissues

All studies utilizing human tissue sources were conducted in accordance with recognized ethical guidelines (Belmont Report and U.S. Common Rule). The LuCaP35CR and LuCaP96CR lines are CX-resistant (CR) prostate cancer PDX models expressing wild-type AR established as part of the University of Washington Medical Center (UWMC) Genitourinary Biorepository as previously described (21). Cell line authentication is regularly performed via STR profiling. Castrated male C.B-17 SCID mice aged 8 to 10 weeks were subcutaneously implanted in bilateral flanks with 30 mm^3 tumor pieces. Tumor volume was measured three times per week and calculated as length $\times$ ($width^2$)/ 2. When tumors reached 200 to 250 mm^3, drinking water was replaced with normal saline supplemented with corticosterone as described above, and mice were randomized to no further treatment (CX alone) or to undergo ADX (CX plus ADX). Tumors from $n = 4$ mice in each PDX model were harvested at 21 to 30 days following ADX. Mice were monitored until tumors reached approximately 1,000 mm^3 (end of study, EOS) or animals became compromised, at which point animals were euthanized according to institutional protocol and tumors harvested for flash freezing and formalin fixation. Because of their prolonged time to tumor regrowth, a subset of mice in the ADX plus CX arms were euthanized and the data censored prior to reaching the size endpoint due to concerns for animal health.

In the LuCaP96CR study, $n = 8$ mice were bilaterally implanted to yield approximately nine evaluable tumors per arm for long term follow-up (~60% take rate). Based on 25% variation in regrowth rates, nine tumors per arm is predicted to provide 80% power with two-tailed α of 0.05 to detect a 35% difference in mean time to regrowth (defined as 750 mm^3). Because of the unexpectedly prolonged time to regrowth following CX plus ADX in this model (with interval attrition of mice due to health reasons) animal number in the combined treatment arm of the LuCaP35CR study was increased to $n = 12$.

Metastatic CRPC tissues for creation of the CRPC tissue microarrays (TMA) were obtained as part of the UWMC Prostate Cancer Rapid Autopsy Program, and comprised metastases from 42 patients (including 65 soft tissue metastases and 120 bone metastases, with up to four metastatic sites from each patient) as previously described (25, 26). The UWMC Institutional Review Board approved all procedures involving human subjects, and all subjects signed written informed consent.

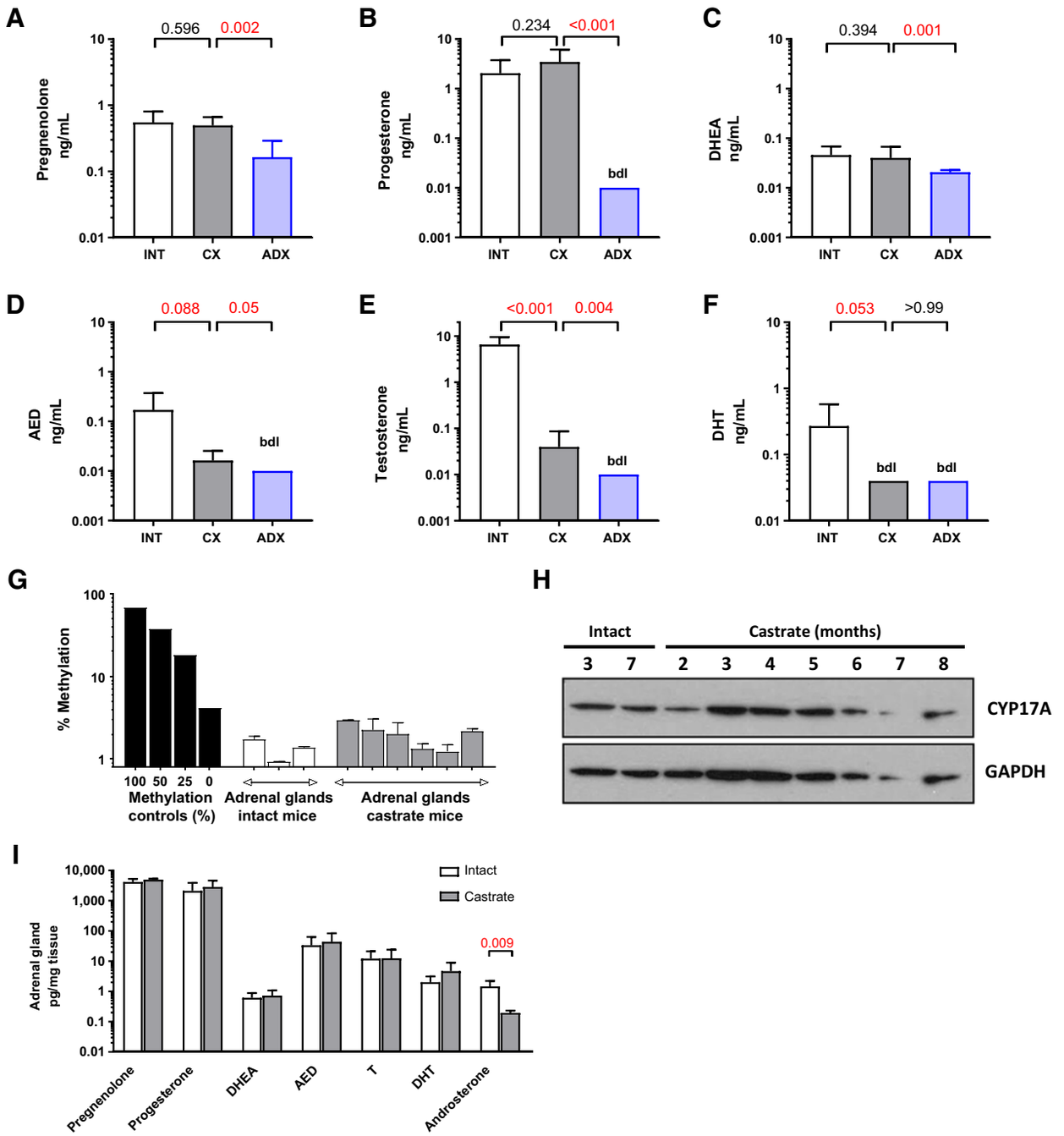

Figure 1.

Serum steroid levels and adrenal CYP17A expression in male C.B-17 SCID mice. **A–F**, Levels of the indicated steroids were measured by mass spectrometry in eugonadal male mice (intact, white bars, $n = 8$) and age-matched mice at 12 weeks after CX alone (gray bars, $n = 7$) or CX + ADX (blue bars, $n = 10$). **G,** Methylation status of CYP17A in adrenal glands resected from intact (age 3 months) and castrated male mice (age 1–3 months), compared with a methylation control ranging from 100% methylated to unmethylated (0%). **H,** Protein levels of CYP17A by Western blot analysis in adrenal glands resected from intact and castrated male mice at the indicated age (in months). **I,** Levels of the indicated steroids in adrenal glands resected from (intact, white bars) and age-matched mice at 12 weeks after CX alone (gray bars). Data in **A–F** and **I** are shown as mean and SD and represent a minimum of six animals per group. *P* values calculated using the Mann–Whitney rank test between the indicated groups (*P* values <0.05 and <0.10 were considered as significant and trending towards significance, respectively).

Pyrosequencing, Western Blotting, and Quantitative RT-PCR

Detailed methods for assessment of adrenal CYP17A methylation status by pyrosequencing, adrenal CYP17A protein expression by Western blotting, and quantitative RT-PCR in murine adrenal glands and xenograft tissues are given in the Supplementary Methods and Supplementary Table S1.

Steroid Measurements

Detailed methods for determination of steroids in serum and tissue samples by mass spectrometry are given in the Supplementary Methods. The lower limits of quantitation (LLOQ) for steroids in serum were 0.01 ng/mL for pregnenolone, progesterone, AED, T, and androsterone; 0.02 ng/mL for DHEA and cortisol, 0.04 ng/mL for DHT and corticosterone, and 0.002 ng/mL for deoxycorticosterone. The LLOQ for steroids in tissue was 0.02 pg/mg for progesterone, AED, DHT, and T; 0.04 pg/mg for DHEA; and 0.08 pg/mg for pregnenolone. Methods for determination of steroids in serum by the Penning Laboratory are as previously published (27).

IHC and Image Analysis

Details for creation of the PDX TMA are given in the Supplementary Methods. The CRPC TMA was created as previously published (26). Detailed methods for immunostaining and specific antibody clones are given in the Supplementary Methods and Supplementary Table S2. Quantitative image analysis of PDX TMA slides stained for AR and ARV7 was performed using metrics we have previously described and further detailed in the Supplementary Methods (28). Scoring for all other stains carried out in a blinded fashion by an experienced pathologist (L.T. or M.T.). A quasi-continuous IHC score was calculated by multiplying each intensity level (0 for no stain, 1 for faint

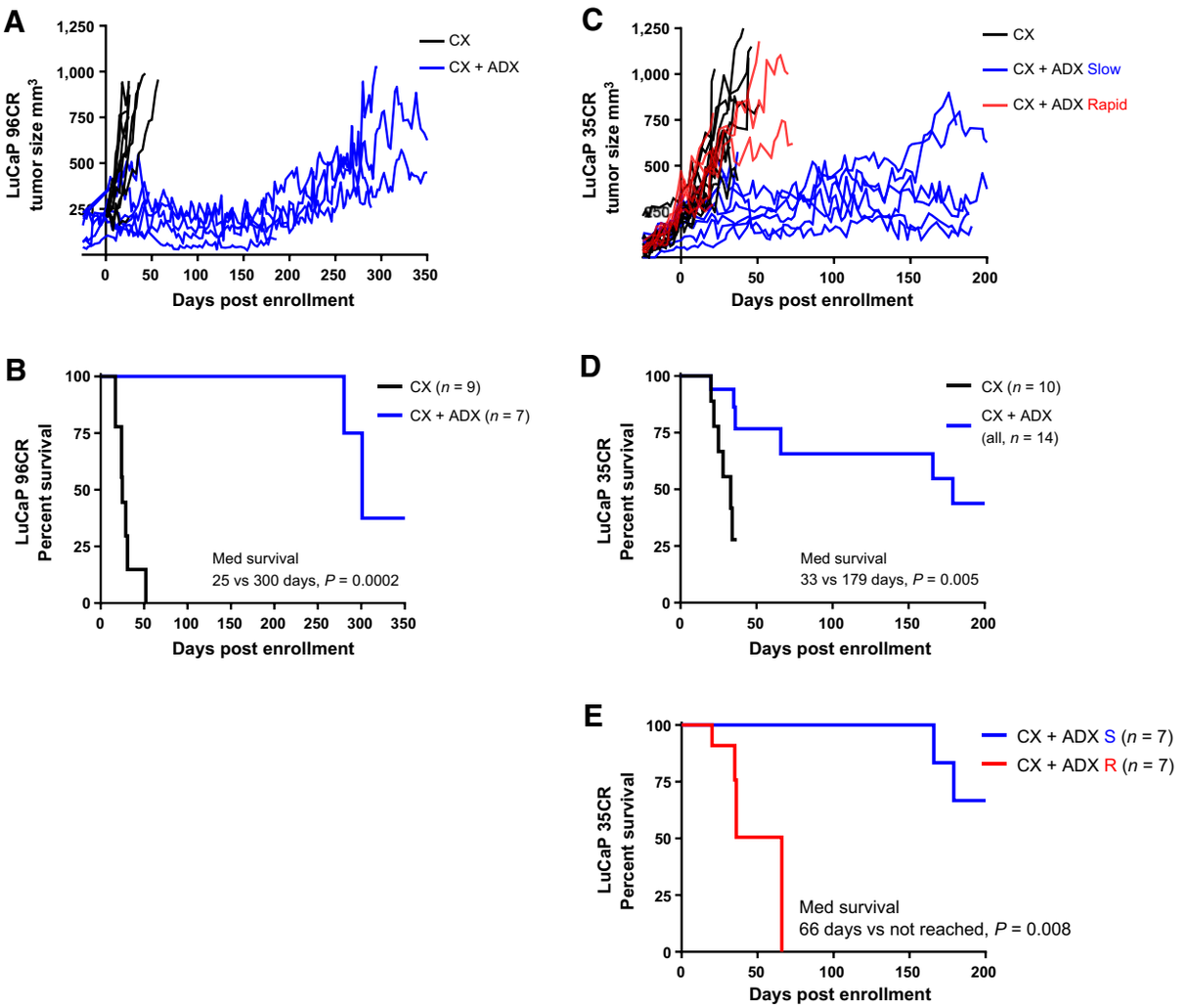

Figure 2.

Impact of ADX on growth of CRPC tumor models *in vivo*. **A,** Individual tumor volume curves for the LuCaP96CR PDX model in mice treated with CX alone (black curves) or CX + ADX (blue curves). **B,** Kaplan–Meier analysis of progression-free survival in CX vs. CX + ADX treated LuCaP96CR tumors (defined as tumor size <750 mm^3) with comparison of curves using the Mantel–Haenszel log-rank test. **C,** Individual tumor growth curves for the LuCaP35CR PDX model in mice treated with CX (black curves) or CX + ADX, among which a subset of tumors regrew slowly (slow, blue curves), whereas a subset (rapid, red curves) regrew with kinetics similar to the CX only group (black curves). **D,** Kaplan–Meier analysis of progression-free survival in CX vs. CX + ADX treated LuCaP35CR tumors. **E,** Kaplan–Meier analysis of progression-free survival in LuCaP35CR tumors treated with CX + ADX, comparing median survival in the tumor subsets with slow (blue) versus rapid (red) regrowth.

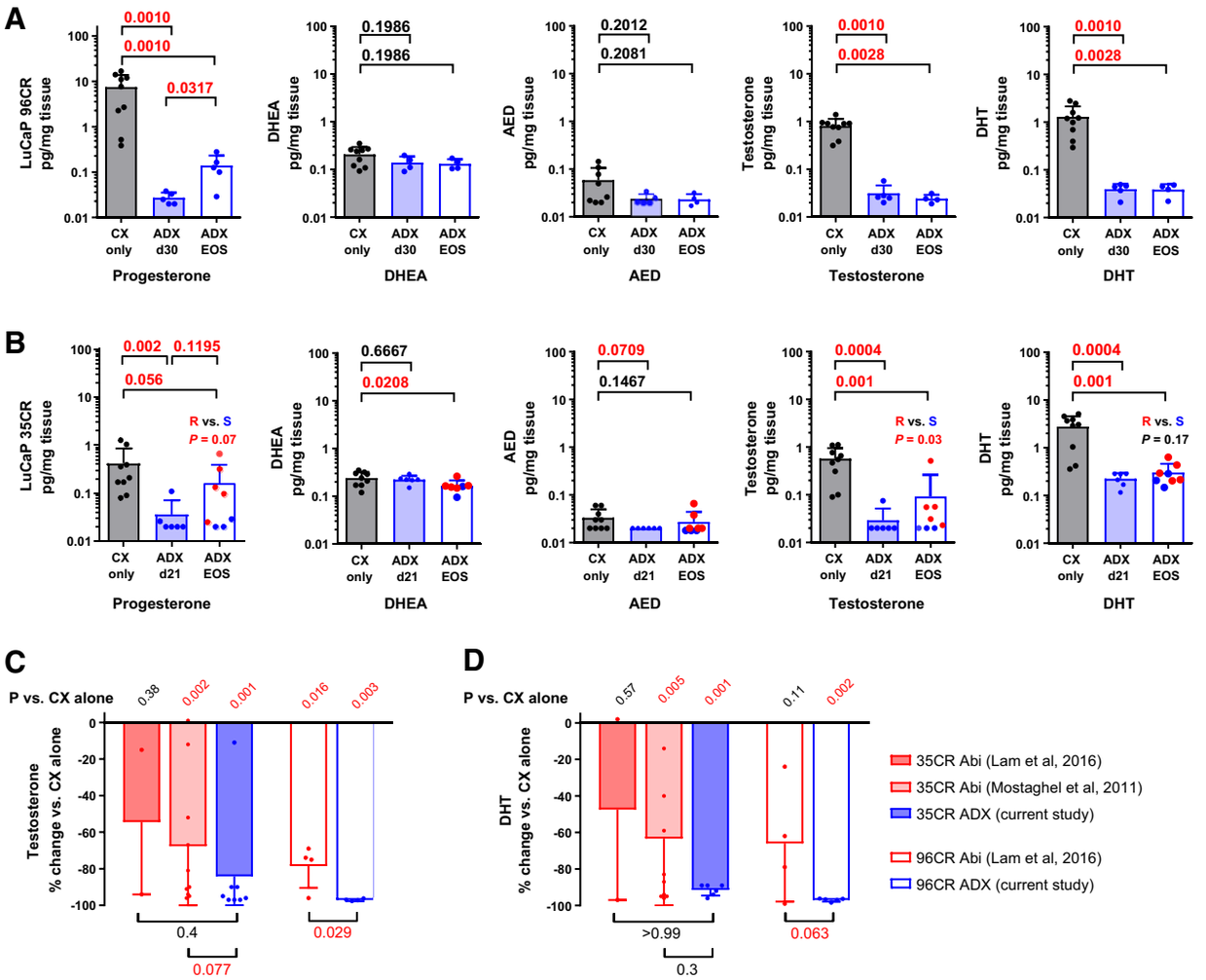

Figure 3.

Impact of adrenal inhibition on tumor steroid levels in CRPC tumor models *in vivo*. Levels of the indicated steroids were measured by mass spectrometry in tumors resected from the (**A**) LuCaP96CR and (**B**) LuCaP35CR PDX studies shown in Fig. 2, in mice treated with CX alone (gray bars) or CX + ADX (blue bars), at short time points (shaded blue bars) or at end of study (EOS, open blue bars). For LuCaP35CR, the subset of EOS tumors that regrew slowly (S, blue dots) versus rapidly (R, red dots) are indicated. Data are shown as mean and SD. *P* values calculated using the Mann–Whitney rank test between the indicated groups (*P* values <0.05 and <0.10 were considered as significant and trending towards significance, respectively). The impact of ABI (red bars, prior studies) versus ADX (blue bars, this study) on the percent change in (**C**) testosterone and (**D**) DHT compared with CX alone is shown for LuCaP35CR (closed bars) and LuCaP96CR (open bars). *P* values for the difference in % change between ABI and ADX treated tumors are given under the horizontal bars at the bottom of each graph. *P* values for the difference in tumor steroids in each treatment group versus Cx alone are given in diagonal font at the top of each graph.

stain, and 2 for intense stain) by the corresponding percentage of cells (0–100%) at the corresponding intensity and totaling the results. For all stains data from the two TMA spots per sample was averaged.

Statistical Analyses

The nonparametric Mann–Whitney rank test was used for all two sample comparisons. *P* values < 0.05 were considered significant and those <0.10 as trending toward significance. Progression-free survival in CX versus CX plus ADX treated mice (defined as tumor size <750 mm^3) was determined via Kaplan–Meier analysis with comparison of curves using the Mantel–Haenszel log-rank test. Statistical analyses were carried out using GraphPad Prism Software.

Results

Impact of ADX on Circulating Steroid Levels in Castrated Mice

To determine the contribution of adrenal androgens to circulating serum levels in castrated mice, we evaluated steroid levels in serum from intact (INT) male C.B-17SCID mice, and from age-matched mice 12 weeks after CX or after CX plus ADX (Fig. 1). As expected, median levels of pregnenolone and progesterone in serum were similar in castrated versus intact mice [0.52 and 0.48 ng/mL pregnenolone, and 1.9 ng/mL vs. 3.2 ng/mL progesterone, p = not significant (ns) for both] and were significantly decreased following ADX [to 0.12 ng/mL, $P = 0.002$ pregnenolone, and to below detectable limits (bdl) for progesterone, $P < 0.001$; Fig. 1A and B], consistent with the

Table 1. Change in transcript levels of AR, AR-regulated genes, GR, and steroidogenic enzymes in CRPC tumors after CX vs. CX + ADX

	LuCaP96CR		LuCaP35CR	
Gene transcript	**Fold**	***P* value[a]**	**Fold**	***P* value[a]**
AR	1.6	ns	3.5	<0.001
V7	4.9	0.005	3.6	0.004
GR (NR3C1)	3.6	0.028	1.6	0.017
PSA	−2.6	0.009	−1.0	ns
TMPRSS2	−1.3	ns	−1.4	ns
FKBP5	2.9	0.068	1.3	ns
CYP17A1	−1.2	ns	−2.1	ns
CYB5A	2.1	0.018	3.8	<0.001
NR5A1	2.1	0.026	3.1	0.001
HSD3B1	1.0	ns	−1.1	ns
AKR1C3	1.3	ns	8.6	<0.001
HSD17B3	−2.1	ns	1.9	0.06
SRD5A1	3.1	0.018	1.8	<0.001
UGT2B15	4.9	0.014	1.4	ns
UGT2B17	−1.4	0.010	Deleted	

[a]*P* values from nonparametric Mann–Whitney test comparing end of study tumors treated with CX alone vs. CX + ADX.

adrenal origin of these steroids. Notably, median levels of DHEA in castrate mice were also similar to those in intact mice (0.03 ng/mL vs. 0.04 ng/mL, p = ns) and decreased to the limit of detection following ADX (to 0.02 ng/mL P = 0.001; Fig. 1C). Following CX median levels of AED and T observed in intact mice were decreased but detectable (from 0.03 to 0.01 ng/mL, P = 0.08 AED; from 1.9 to 0.02 ng/mL, $P < 0.001$ T), only becoming undetectable following ADX ($P = 0.05$ and 0.004, respectively; Fig. 1D and E), whereas levels of DHT in intact mice (0.15 ng/mL) became undetectable following CX alone ($P = 0.05$; Fig. 1F). Serum levels of DHEA, AED, T, and DHT from a separate cohort of intact and 6-week castrated male C.B-17 mice, were independently measured in the laboratory of Dr. Penning, and were consistent with our measurements, with the higher castrate T levels in the latter likely reflecting the shorter duration of CX (Supplementary Table S3).

Consistent with literature documenting corticosterone as the primary circulating mineralocorticoid in mice (13, 14), circulating levels of cortisol were undetectable (not shown), whereas levels of 11-deoxycorticosterone were similar in intact and castrated mice (2.6 ng/dL vs. 4.8 ng/mL, p = ns) and became significantly decreased following ADX (0.005 ng/dL, $P < 0.001$; Supplementary Fig. S1A). Because of the requirement for mineralocorticoid replacement (administered as corticosterone in drinking water), levels of corticosterone in the adrenalectomized mice were similar to those in the intact and castrated mice; Supplementary Fig. S1B).

Expression of CYP17A and Steroid Levels in Adrenal Glands of Castrated Mice

Previously published data in rats and in the mouse adrenocortical Y1 cell line suggested epigenetic regulation of CYP17A expression in adrenal cells via methylation, possibly via activity of cAMP responsive element modulator (CREM) isoforms (29–31). However, we show that CpG islands in the *CYP17A* promoter DNA were unmethylated (Fig. 1G) and protein expression was detectable by Western blot analysis (Fig. 1H) in adrenal glands of intact and castrated mice ranging in age from 12 to 36 months (3–8 months; to mirror the ages spanning the course of a typical xenograft study). Transcripts of steroidogenic genes required for *de novo* and adrenal androgen synthesis (Star, Cyp11a, Cyp17a, Hsd3b1) and of Srd5a (required for production of DHT) were detectable in adrenal glands of intact mice and were significantly increased after CX (Supplementary Fig. S1C), as observed previously in some rodent studies (19, 32, 33). Notably, adrenal expression of melanocortin 2 receptor (Mc2r; also known as adrenocorticotropic hormone receptor; Acth) was also increased following CX, and is consistent with response to Acth as a driver of adrenal steroidogenesis in the castrate setting (sufficient serum for ACTH measurements was not available).

To confirm the functional significance of adrenal steroidogenic enzyme expression, we evaluated steroid levels in adrenal glands resected from eugonadal mice and age-matched castrated mice (12 weeks after CX; Fig. 1I). As expected, median levels of pregnenolone (4,238 pg/mg) and progesterone (1,876 mg/pg) were very high in adrenal glands of intact mice and remained unchanged by CX. Notably, median levels of AED (24.6 pg/mg) and T (10 pg/mg) in adrenal glands from intact mice were substantial, while levels of DHEA (0.7 pg/mg), DHT (1.7 pg/mg), and androsterone (1.4 pg/mL) were easily measurable. Similar to pregnenolone and progesterone, adrenal levels of AED, T, and DHT were also unchanged by CX, suggesting that testicular steroids do not serve as a source of these androgens detected within the adrenal gland. In contrast, median levels of androsterone in the adrenal gland were substantially decreased after CX, suggesting a testicular contribution to this steroid level (P = 0.095).

As serum androgen levels in castrated mice may be influenced by steroid production in other organs with steroidogenic potential, we assessed steroid levels in liver, kidney and muscle (Supplementary Fig. S2; refs. 34, 35). Notably, levels of pregnenolone, progesterone, AED, T, and DHT in the adrenal gland of castrated mice were 2–3 orders of magnitude higher than levels in liver, kidney and muscle (Supplementary Fig. S2A–S2F), suggesting active production specific to the adrenal gland. Moreover, while CX did not affect steroid levels in the adrenal gland (other than androsterone), it significantly decreased levels of AED in liver ($P = 0.10$; Supplementary Fig. S2D), of T in liver, kidney and muscle ($P = 0.013$, 0.05, 0.028; Supplementary Fig. S2E), of DHT in kidney (P = 0.028; Supplementary Fig. S2F), and of androsterone in liver (P = 0.039; Supplementary Fig. S2G). These observations demonstrate

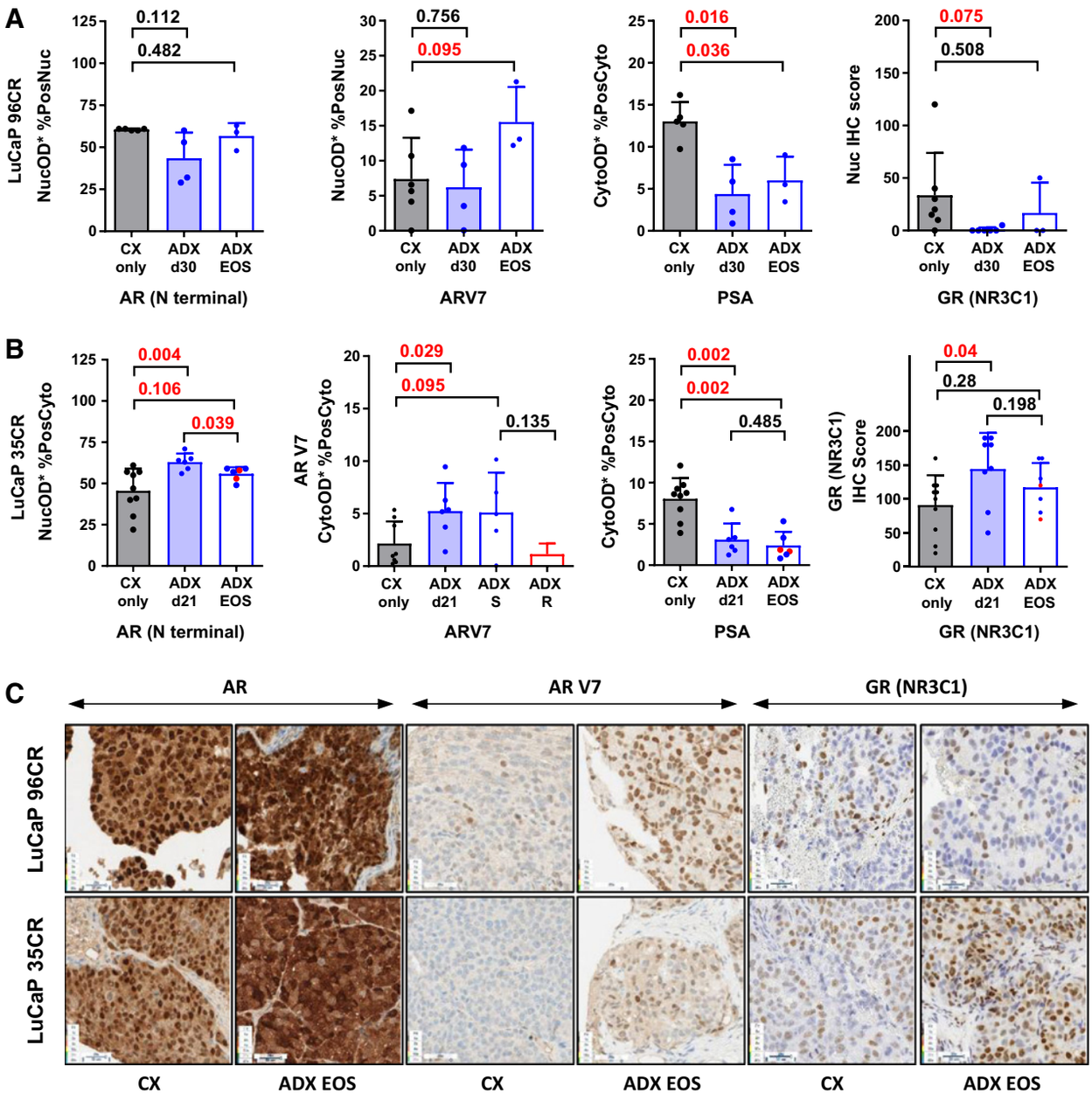

Figure 4.

Impact of ADX on IHC staining for AR, ARV7, PSA, and GR in CRPC tumor models *in vivo*. IHC staining for the indicated protein in tumors resected from the (**A**) LuCaP96CR and (**B**) LuCaP35CR PDX studies shown in Fig. 3 in mice treated with CX alone (gray bars) or CX + ADX (blue bars), at short time points (shaded blue bars) or at end of study (EOS, open blue bars). For LuCaP35CR, the subset of EOS tumors that regrew slowly (S, blue dots) versus rapidly (R, red dots) are indicated. Staining for AR, ARV7, and PSA quantified as the average nuclear (AR, ARV7) or cytoplasmic (PSA) staining intensity within tumor epithelium multiplied by the percentage of positive nuclei (AR, ARV7) or cells with positive cytoplasm (PSA) in tumor epithelium (denoted as AvgNuclearOD*%PosNuclei or AvgCytoOD*%PosCyto). Semiquantitative scoring for nuclear GR expression calculated by multiplying the intensity level (0 for no stain, 1 for faint stain, and 2 for intense stain) by the percentage of cells (0–100%) at each intensity level and totaling the results, ranging from 0 (no staining in any cell) to 200 (intense staining in 100% of the cells). Data are shown as mean and SD. *P* values calculated using the Mann–Whitney rank test between the indicated groups (*P* values <0.05 and <0.10 were considered as significant and trending towards significance, respectively). **C,** Representative examples of the indicated stains for LuCaP96CR (top) and LuCaP35CR (bottom) PDX models, showing each stain in an EOS tumor from a CX only or CX + ADX treatment arm.

the testicular contribution to steroid levels detected in liver, kidney, and muscle, and support the hypothesis that circulating steroid levels observed in castrated mice are primarily derived from the adrenal gland rather than other organs.

Impact of ADX on Tumor Growth and Steroid Levels in CX-Resistant PDX Models

To evaluate the functional relevance of adrenally-derived steroids in CRPC tumor models *in vivo*, we determined the impact of

ADX on suppressing tumor growth and intratumoral androgens in the LuCaP96CR and LuCaP35CR PDX models in castrated C.B-17 SCID mice. In the LuCaP96CR PDX model (Fig. 2A), tumor regrowth was markedly delayed by CX plus ADX (CX + ADX, blue curves) compared with CX alone (CX, black curves), with an increase in median survival (to tumor endpoint of 750 mm^3) from 25 days (in the CX group) to 300 days (in the CX + ADX group; $P = 0.0002$; Fig. 2B). In the LuCaP35CR model (Fig. 2C), tumor growth was markedly delayed by CX + ADX in a subset of tumors (slow, blue curves), whereas a subset (rapid, red curves) regrew with kinetics similar to the CX only group (black curves). Median survival in the CX only versus the entire CX + ADX cohort was delayed from 33 to 179 days ($P = 0.005$; Fig. 2D), with the growth prolongation primarily contributed by the slow subset of tumors (median survival not reached vs. 66 days in the Rapid group, $P = 0.008$; Fig. 2E).

In LuCaP96CR median intratumor levels of pregnenolone, progesterone, T, and DHT were decreased by an order of magnitude at 30 days after ADX + CX (ADX d30) compared with CX alone (pregnenolone 24.3 pg/mg vs, 2.7 pg/mg, $P = 0.008$ (not shown); progesterone 1.4 pg/mg vs. 0.03 pg/mg, $P = 0.001$; T 0.9 pg/mg vs. 0.03 pg/mg, $P = 0.001$; DHT 1.2 pg/mg vs. 0.03 pg/mg, $P = 0.001$; Fig. 3A). Tumor levels of DHEA and AED were lower at ADX d30 versus CX alone, although the decreases did not reach statistical significance (p = ns for both). Although levels of DHEA, AED, T, and DHT remained suppressed near the limit of detection in the end of study (EOS) tumors that regrew after CX + ADX (ADX EOS), progesterone levels in these EOS tumors were increased compared with tumors resected at day 30 after ADX (0.03 pg/mg vs. 0.125 pg/mg, $P = 0.0317$), although still lower than tumors in the CX only group.

In LuCaP35CR median intratumor levels of progesterone, T and DHT were also decreased by an order of magnitude by 21 days after ADX (ADX d21) compared with CX alone (progesterone 0.21 pg/mg vs. 0.02 pg/mg, $P = 0.002$; T 0.6 pg/mg vs. 0.02 pg/mg, $P = 0.0004$; DHT 3.2 pg/mg vs. 0.25 pg/mg, $P = 0.0004$; Fig. 3B), whereas decreases in AED trended toward significance (0.03 pg/mg vs. 0.02 pg/mg, $P = 0.07$, respectively). Steroid levels in tumors that regrew after CX + ADX (ADX EOS) were significantly below those in the CX alone group for progesterone, DHEA, T, and DHT ($P = 0.056$, 0.02, 0.001, and 0.001, respectively); however, median levels in tumors that regrew rapidly (red dots in Fig. 3B) trended toward being higher than levels in tumors that regrew slowly (blue dots) for progesterone ($P = 0.07$), T ($P = 0.03$), and DHT ($P = 0.17$), suggesting the more rapid regrowth in these tumors was in part stimulated by the elevation in tumor androgens. In both models, serum androgens levels following ADX were largely below detectable limits (not shown), precluding assessment of correlation with tumor androgens.

Notably, surgical ADX showed a significantly more profound impact on suppressing tumor androgens and CRPC tumor growth than did previously published studies from our group using ABI, in which LuCaP96CR was classified as an intermediate responder, and LuCaP35CR showed no response in one study and moderate response in another (18, 36). Compared with these studies, ADX more consistently suppressed tumor levels of pregnenolone, progesterone, DHEA, and AED (blue bars, Supplementary Fig. S3A–S3D) than did ABI (red bars), whereas in at least in one model (LuCaP35CR) ABI was associated with increases in pregnenolone and progesterone (immediately upstream of the first enzymatic function of CYP17A inhibited by ABI), and DHEA (immediately upstream of HSD3B1, which is also inhibited by ABI; ref. 37). Similarly, ABI clearly suppressed EOS levels of T and DHT (red bars, Fig. 3C and D); however, ADX (blue bars) appeared to do so more consistently.

Induction of AR, ARV7, and GR in ADX-Resistant CRPC

We determined the impact of ADX on key mechanisms of resistance identified in treatment refractory CRPC including expression of AR, the prevalent AR splice variant—ARV7, glucocorticoid receptor (GR, NR3C1) and steroidogenic enzymes, as potential mechanisms driving tumor re-growth under the stringent suppression of ligand levels observed in the setting of CX + ADX (3, 18, 36).

In LuCaP96CR, we observed no change in transcript levels of *AR*, but a significant induction of *ARV7* (4.9-fold, $P = 0.005$), decrease in *PSA* (−2.6-fold, $P = 0.009$), and increase in expression of *GR* (3.6-fold, $P = 0.028$) in the EOS tumors (Table 1). IHC staining of a TMA created from this PDX model (Fig. 4A) similarly showed no change in AR following ADX, an increase in nuclear ARV7 staining ($P = 0.08$ at EOS, $P = 0.05$ for EOS vs. ADX d30), and a decrease in cytoplasmic PSA ($P = 0.016$ at ADX d30, $P = 0.035$ at EOS). However, an increase in nuclear GR staining was not observed, which instead showed an apparent decrease ($P = 0.025$ at ADX d30). These data suggest induction of ARV7 as a significant mechanism of resistance in this PDX model, potentially accounting for the observation that transcript levels of some androgen regulated genes (e.g., *TMPRSS2* and *FKBP5*) were not necessarily decreased in the EOS tumors.

In LuCaP35CR, we observed a significant induction of *AR* (3.5-fold, $P \leq 0.001$), *ARV7* (3.6-fold, $P = 0.004$), and *GR* message (1.6-fold, $P = 0.017$) in the EOS tumors (Table 1). There was no change in the androgen-regulated genes *PSA*, *TMPRSS2*, or *FKBP5* at the transcript level in this PDX model, although IHC staining (Fig. 4B) did show a decrease in cytoplasmic PSA (at ADX d21 and at EOS, $P = 0.0016$ for both). Consistent with the transcript results, we observed an increase in nuclear AR, ARV7, and GR staining in this model (Fig. 4B) that was moderately more significant at ADX d21 ($P = 0.004$, 0.029, and 0.025, respectively) than in the EOS tumors ($P = 0.106$, 0.095, and 0.15, respectively). We did not observe significant differences in AR, PSA, or GR staining in the EOS tumors that re-grew rapidly (red dots, Fig. 4B) versus those that regrew slowly (blue dots). However, the increase in ARV7 seen at ADX d21 is appeared to be sustained in the EOS tumors that recurred with low androgen levels (blue dots, here and in EOS T and DHT levels, Fig 3B), but not in the EOS tumors that recurred with an increase in tumor androgens (red dots, here and in EOS T and DHT levels, Fig. 3B). These data suggest induction of AR, ARV7, and GR as potentially significant mechanism of resistance in this model, with ARV7 playing a more important role in tumors that regrew without an increase in intratumoral androgen levels, consistent with the known inverse relationship between androgen levels and ARV7 expression (38). Of note, corticosterone supplementation itself had no impact on tumor growth (Supplementary Fig. S4A) or IHC expression of GR (Supplementary Fig. S4B) or of AR and ARV7 (not shown). This suggests the induction of GR expression in the ADX-treated tumors in this model reflects the impact of ADX and not the replacement corticosterone dosing.

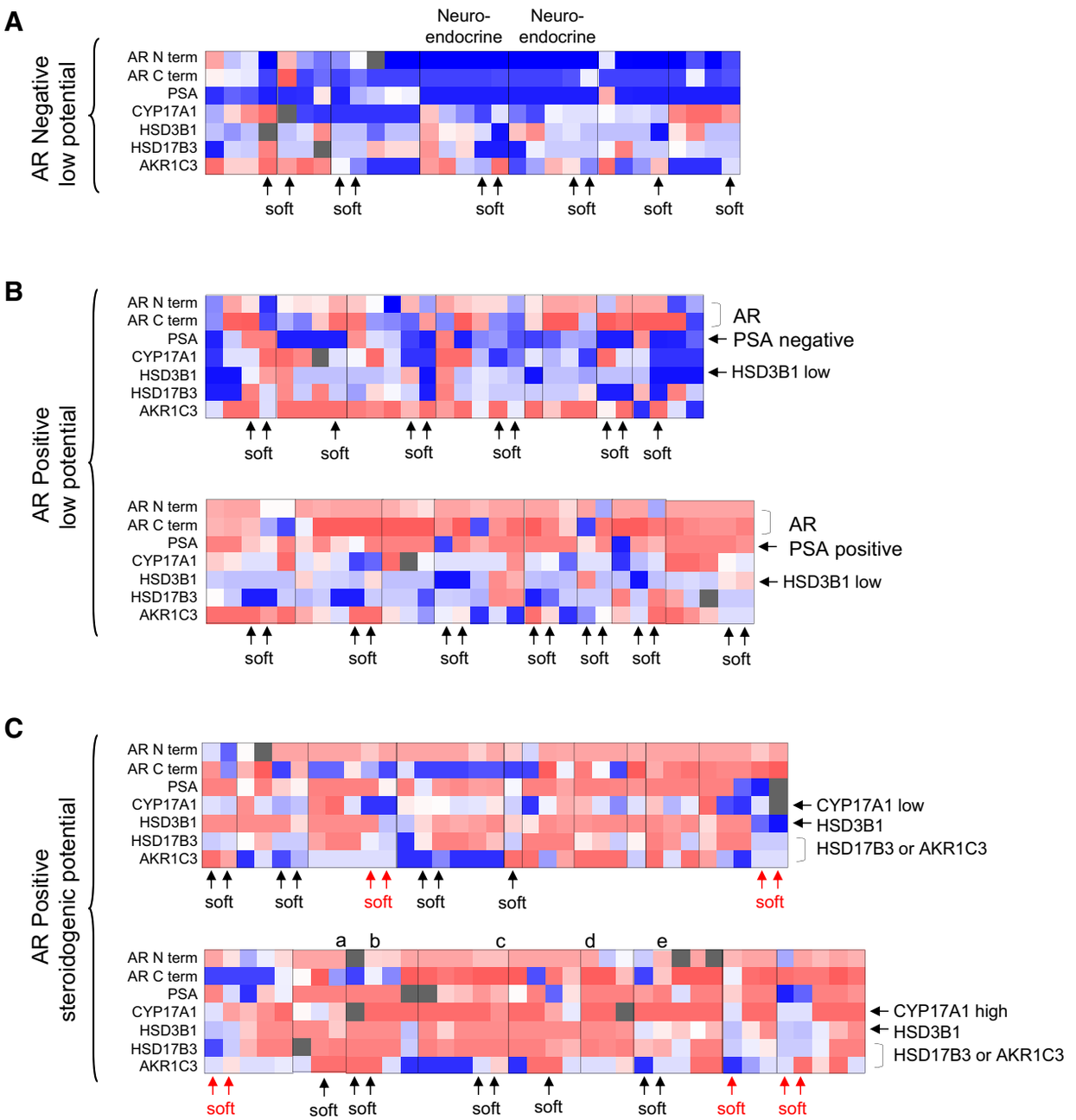

Figure 5.

Expression of steroidogenic enzymes in CRPC metastases. The heatmap summarizes staining observed on a TMA containing multiple bone and soft tissue CRPC metastases from 43 men collected via rapid autopsy. Each column represents serial staining of the same metastasis for the indicated proteins, ranging from absent expression (dark blue) to high expression (dark red). Vertical lines demarcate the set of metastases from each patient. Tumors are grouped based on negative (**A**) or positive (**B, C**) AR expression (in the majority of tumors in an individual patient), and then by steroidogenic potential. **A,** AR negative tumors with negative PSA staining and low expression of steroidogenic enzymes. Tumors from the two patients indicated had neuroendocrine histology. **B,** AR positive tumors with negative (top) or positive (bottom) PSA expression and low steroidogenic potential (based on low HSD3B1 expression). **C,** AR positive tumors with high steroidogenic potential. Tumors are grouped based on potential for adrenal androgen conversion (coordinate expression of HSD3B1 and HSD17B3/AKR1C3 with low CYP17A1, top), or potential for *de novo* steroidogenesis (coordinate expression of CYP17A1, HSD3B1, and HSD17B3/AKR1C3, bottom). Among the group with high steroidogenic potential, patients in whom the soft tissue metastases appear distinctly different than the bone metastases are indicated in red. Representative IHC stains of the metastases labeled a to e in **C** are shown in Supplementary Fig. S6.

Induction of Steroidogenic Enzyme Expression in ADX-Resistant CRPC

Consistent with the increased intratumoral levels of T and DHT observed in a subset of the ADX recurrent LuCaP35CR tumors (red dots, Fig. 3B), we observed increased expression of several genes involved in mediating steroidogenic enzyme activity (Table 1; see Supplementary Fig. S5 for schema of androgen biosynthesis enzymes), including *CYB5A* (enhances activity of CYP17A and HSD3B, 3.8-fold $P < 0.001$), *NR5A1* (transcriptional regulator of multiple steroidogenic genes, 3.1-fold $P = 0.001$), *AKR1C3* (8.3-fold $P < 0.001$), HSD17B3 (1.9-fold $P = 0.06$), and *SRD5A1* (1.8-fold $P < 0.001$; refs. 39, 40). In contrast, although ADX EOS tumors in the LuCaP96 model also showed increases in expression of *CYB5A1* and *NR5A1* (two-fold for both, $P = 0.018$ and 0.026, respectively) and *SRD5A1* (3.1-fold $P = 0.018$), they did not show induction of the steroid producing genes *AKR1C3* or *HSD17B3* but rather induction of *UGT2B15* (4.9-fold $P = 0.014$), which conjugates T and DHT for excretion, potentially explaining the differences in androgen levels observed in the two models.

Expression of Steroidogenic Enzyme in CRPC Metastases

To further assess the translational relevance of the steroidogenic enzyme transcripts observed in the ADX-treated tumors, we evaluated AR axis proteins (AR, PSA) and key enzymes required for *de novo* steroid synthesis and/or conversion of adrenal androgens (HSD3B1, CYP17A1, AKR1C3, and HSD17B3; Supplementary Fig. S5) in a TMA of bone and soft tissue CRPC metastases from 43 patients (two to six metastases per patient). Despite some degree of intrapatient heterogeneity, grouping of tumors by patient of origin revealed several distinct staining profiles, including subsets of patients with (i) AR^- and PSA^- tumors with low expression of steroidogenic enzymes (Fig. 5A), (ii) AR^+ tumors with negative (Fig. 5B top) or positive (Fig. 5B bottom) PSA expression and low steroidogenic potential (based on generally low expression of HSD3B1, which is required for both *de novo* synthesis and conversion of adrenal androgen), and (iii) AR^+ and PSA^+ tumors with high steroidogenic potential (Fig. 5C, based on moderate to high expression of HSD3B1). Tumors in the latter group can be further subdivided based on potential for adrenal androgen conversion [e.g., coordinate expression of HSD3B1, HSD17B3/AKR1C3 (which catalyze the same reaction) but low CYP17A1; Fig. 5C, top], or potential for *de novo* steroidogenesis (e.g., coordinate expression HSD3B1, HSD17B3/AKR1C3, and high CYP17A; Fig. 5C, bottom). Representative images of tumors showing coordinate expression of HSD3B1, HSD17B3/AKR1C3, and CYP17A are shown in Supplementary Fig. S6. As we have previously published, a subset of these tumors show loss of C terminal AR staining, consistent with the presence of truncated AR variant species (41).

Discussion

Clinical studies of ABI in men with metastatic prostate cancer are consistent with an important role for CYP17A-mediated adrenal androgen production in CRPC progression, particularly as higher pretreatment levels of circulating adrenal androgens associate with better response to CYP17A inhibition (42–44). However, inhibition of intratumoral CYP17A activity is not excluded, and ABI and its metabolites can directly target the AR (12). Thus, these studies do not actually isolate the specific contribution of adrenal steroids in CRPC progression. It has been widely held that rodent adrenal glands do not produce adrenal androgens and that rodent models cannot, therefore, be used to test this facet of prostate cancer biology. We now show that adrenal CYP17A is present in C.B-17 SCID mice, that steroids downstream of CYP17A are detectable in the adrenal glands and serum of castrated mice, and that surgical ADX markedly suppresses serum and tumor steroid levels and delays tumor regrowth beyond that observed with CX alone in two PDX models of CRPC. This is the first study to demonstrate the specific impact of adrenal steroids on intratumoral androgens and CRPC tumor growth *in vivo*.

Functional CYP17A is transiently present in rodent adrenal glands during the fetal/early postnatal period (45, 46) and then decreases, likely via epigenetic methylation and repression (29). This phenomenon is not universal however, as we show that adrenal *CYP17A* DNA is unmethylated and detectable in C.B-17 SCID mice, consistent with the spiny mouse (Acomys cahirinus) that is known to express functional CYP17A (46). Gonadectomy induces adrenal gland expression of steroidogenic genes and increases circulating levels of AED and T in certain inbred mouse strains (33). We did not observe differences in CYP17A methylation status or in transcript and protein levels between intact and castrated mice, although we did observe statistically significant increases in transcript expression of *STAR*, *CYP11A*, *HSD3B1*, and *SRD5A2* at 12 weeks following CX.

Importantly, we show levels of adrenal androgens (DHEA, AED) and downstream metabolites (T, DHT, and androsterone) are easily detectable in adrenal glands of intact mice and do not decrease following CX. The adrenal levels of DHEA (0.7 pg/mg, range 0.44–1.2 pg/mg) and AED (44 pg/mg, range 4–97 pg/mg) in our study are consistent with the findings of Hu and colleagues who reported levels of DHEA (~4–7 pg/mg) and AED (~2–4 pg/mg) in the adrenal glands of rats (Wistar, via GC/MS) 8 weeks after CX, equivalent to levels in intact rats (23). Moreover, we show adrenal levels of AED, T, and DHT in castrated mice to be nearly 2 orders of magnitude higher than in kidney, liver, or muscle (other organs shown to have steroidogenic capacity in mice; refs. 34, 35), suggesting active production specific to the adrenal gland.

An existing body of data, published primarily in the endocrine literature and not well-recognized in the prostate cancer field, supports functional adrenal CYP17A activity in adult rodents and may reflect strain-specific differences. Although some rodent adrenal suspension studies failed to detect production of 17-hydroxyprogesterone or AED (products of CYP17A hydroxylase and lyase activity, respectively) via RIA (13), others did measure AED or DHEA (via RIA; refs. 46, 47) or showed metabolism of [3H]DHEA or [3H]AED to T and DHT *in vitro* (48, 49). Similarly, serum levels of T, DHT, and AED were undetectable in some strains of castrated rats (Holtzmann, via RIA; ref. 50); Wistar, via LC/MS; ref. 51), but detectable in others (Sprague–Dawley, via LC/MS (19, 52). Kyprianou and Isaacs detected circulating (T 0.10 ng/mL and DHT 0.16 ng/mL) and prostatic levels of T and DHT (via RIA) in castrated Copenhagen rats that were eliminated by ADX (22), although a study in Wistar rats showed a decrease in prostate levels of T and DHT after CX but no sustained decrease in AED or DHEA (via GC/MS), consistent with an adrenal origin (23). In context of this study, the relevance of this literature becomes more apparent and provides significant support for our findings.

Strain-specific differences in adrenal androgen production are suggested by the observation that certain inbred strains of mice (DBA/2J, CE/J, C3H, NU/J, BALB/c, and B6D2F1) are highly sensitive to gonadectomy induced sex-steroid producing adrenocortical neoplasia, whereas others (C57BL/6 and FVB/N) are not (53). The mouse strains associated with adrenal androgen production in the literature are consistent with those susceptible to adrenal neoplasia, with androgens observed in BALB/c mice (via RIA; ref. 13) but not in C57BL/6 mice (via LC/MS; ref. 54). In this respect it is notable that the C.B-17 SCID mice used in our study are derived from the BALB/C strain.

Notably, surgical ADX showed a significantly more profound impact on suppressing tumor androgens and CRPC tumor growth than did previously published studies from our group using ABI (18, 36). Although ABI clearly suppressed EOS levels of T and DHT in the prior studies (red bars, Fig. 3C and D), ADX (blue bars) appeared to do so more consistently. Differences in growth suppression might also reflect the AR agonist activity attributed to a 5α reduced metabolite of ABI (55), an effect that would be absent in the ADX-treated tumors.

Given the clear impact of both ADX and ABI on tumor androgen levels, we sought to determine whether mechanisms of resistance to ADX mirrored those observed with ABI. Consistent with our previous findings in LuCaP96CR tumors treated with ABI (36), we observed increased transcript levels of *ARV7* and *GR*, and no increase in transcript or nuclear staining for full-length *AR* in the ADX-treated tumors (although we did not observe increased nuclear expression of *GR* as noted in that study). In LuCaP35CR tumors, we observed increased transcript expression and nuclear staining of AR and ARV7 and an increase in nuclear GR staining after ADX, consistent with prior data (although increased AR expression was only observed in one of the prior studies likely due to PDX heterogeneity; refs. 18, 36). These data suggest induction of ARV7 as a potentially significant mechanism of resistance following ADX in LuCaP96CR, and induction of AR, ARV7, and GR as potentially significant mechanisms of resistance in LuCaP35CR. Although AR and ARV7 share an overlapping transcriptome, transcripts of AR target genes are not consistently increased in the ADX-treated tumors, consistent with prior observations that ARV7 is not necessarily as potent as full-length AR in inducing the expression of canonical AR genes (56, 57).

Our data suggest that the adrenal gland contributes substantially to levels of T and DHT in CRPC tumors grown in castrated mice, and is consistent with our data demonstrating expression of enzymes required for adrenal androgen utilization in a majority of AR+ CRPC metastases examined (Fig. 5C). However, a subset of ADX-resistant LuCaP35CR tumors demonstrate induction of steroidogenic enzymes and moderate reconstitution of intratumoral progesterone, T and DHT (similar to our prior data in ABI-recurrent LuCaP35CR tumors (18). These suggest that at least some tumor models are also capable of *de novo* steroid production and is consistent with the concurrent expression of enzymes required for *de novo* steroidogenesis in a subset of the CRPC tumors we evaluated (Fig. 5C, bottom). As increased progesterone levels were present in a subset of the ADX EOS tumors versus earlier time points in both PDX models, we determined whether these EOS tumors showed induction of the progesterone receptor (PR) as possible mechanism of progression (58). However, staining for PR was low to undetectable in the CX only tumors, without any difference in the ADX-treated tumors (data not shown). A direct effect of progesterone on stimulation of growth via wild-type (WT) AR cannot necessarily be excluded, as Kumagai et al. did not detect downstream conversion of progesterone to T or DHT in VCaP cells (which has WT AR), yet still observed modest activation of growth (59). Activation of WT AR by a metabolite directly downstream of progesterone (20β-hydroxy-5α-dihydroprogesterone) has also been recently demonstrated (60). We did not measure levels of this particular steroid in our assay, but as its production from progesterone is not mediated by CYP17A it suggests another reason why surgical ADX appears to have better anti-tumor efficacy than CYP17A inhibition with ABI.

We and others have previously demonstrated transcript expression of steroidogenic enzymes in subsets of CRPC metastases, but data on concordant protein expression of key enzymes required for androgen synthesis from adrenal androgens or earlier precursors are limited (2, 3, 61–66). Here, we demonstrate clear subsets of tumors with coordinate expression of the critical enzymes required for *de novo* steroid synthesis and/or conversion of adrenal androgens. Steroidogenic enzyme expression is generally low in AR negative tumors (Fig. 5A), and in AR positive tumors with low PSA expression (Fig. 5B, top), indicative of poor response to agents targeting the AR or ligand synthesis. Low expression of steroidogenic enzymes is also observed in a subset of AR and PSA positive tumors (Fig. 5B, bottom), suggesting AR axis signaling in response to exogenous ligand is maintained, but without intratumoral androgen production. In contrast, tumors from nearly half the patients (Fig. 5C) appear potentially capable of androgen production from adrenal androgens (based on concordant expression of HSD3B1 with AKR1C3 or HSD17B3,), and of these, half also show concordant expression of CYP17A (Fig. 5C, bottom), suggesting capacity for *de novo* steroidogenesis.

Although we did not observe consistent differences in steroidogenic capacity between bone and soft tissue tumors overall, there was more pronounced staining in bone versus soft tissue metastases in several patients (red arrows in Fig. 5C), potentially consistent with the observation that osteoblasts may induce steroidogenic enzymes in CRPC cells (67). Unexpectedly, some tumors with loss of C terminal AR staining (consistent with the presence of ligand-independent AR variants) also demonstrated steroidogenic enzyme expression, suggesting that in certain cases the response to CX may include both induction of AR variants and upregulated steroid production. Alternatively, ARV7 is a strong inducer of the glucuronidating enzyme UGT2B17, which conjugates active androgens for excretion, and could therefore continue to promote AR variant production in the presence of concomitant steroidogenesis (41).

In summary, we show that adrenally-derived steroids are produced in C.B-17 SCID mice and contribute to tumor androgen levels and growth in two PDX models of CRPC, demonstrating that C.B-17 SCID mice are an appropriate model for evaluating the impact of steroidogenesis inhibitors in CRPC xenograft studies. Although the potential impact/availability of low circulating T levels may be magnified in mice compared with humans due to the lack of circulating sex hormone binding globulin (SHBG) in mice (68), castrate levels of DHEA, AED, T, and DHT in this study were similar to those in ABI-treated CRPC patients (as previously reported for T; ref. 68). These suggest a reduction in adrenally-derived androgens beyond those achieved by ABI may have clinical benefit in men with CRPC, and is consistent with our observation that tissue androgens and tumor growth were suppressed more strongly by surgical ADX in this study than in previously reported studies using ABI. These suggest that proof-

of-concept studies testing agents capable of achieving true "non-surgical ADX" are warranted (such as the recently reported CYP11A inhibitor ODM-208; ref. 69) and that optimal clinical efficacy may be obtained by a combination of CYP11A and CYP17A inhibition. Although beyond the scope of the current work, PDX studies testing CYP11A inhibition are planned. We find that mechanisms of resistance after surgical ADX in CRPC models are similar to those observed following ABI, including the induction of AR, truncated AR splice variants, GR, and steroidogenesis. This is consistent with the fact that both approaches act via suppression of tissue androgen levels, and suggests optimal clinical activity will be achieved by combination strategies cotargeting AR or GR with agents capable of fully abrogating adrenal and intratumoral ligand synthesis.

Disclosure of Potential Conflicts of Interest

E.A. Mostaghel is a consultant/advisory board member for Orion Pharma. T.M. Penning reports receiving other commercial research support from Forendo, receiving speakers bureau honoraria from Congress Steroid Research, holds ownership interest (including patents) in Penzymes, and is a consultant/advisory board member for Markey Cancer Center, Research Institute for Fragrance Materials, CounterAct-Rutgers University, Columbia University SPH, and Berkeley U-Superfund Research Program. No potential conflicts of interest were disclosed by the other authors.

Authors' Contributions

Conception and design: E.A. Mostaghel, S.P. Balk, P.S. Nelson
Development of methodology: E.A. Mostaghel, A. Zhang, D. Tamae, M. Tretiakova, R. Dumpit, T.M. Penning, E. Corey, L.D. True, P.S. Nelson
Acquisition of data (provided animals, acquired and managed patients, provided facilities, etc.): E.A. Mostaghel, A. Zhang, S. Hernandez, B.T Mark, D. Tamae, J. Bartlett, J. Burns, L. Ang, A.M. Matsumoto, T.M. Penning, C. Morrissey
Analysis and interpretation of data (e.g., statistical analysis, biostatistics, computational analysis): E.A. Mostaghel, A. Zhang, X. Zhang, D. Tamae, H.E. Biehl, M. Tretiakova, A.M. Matsumoto, L.D. True, P.S. Nelson
Writing, review, and/or revision of the manuscript: E.A. Mostaghel, A. Zhang, D. Tamae, M. Tretiakova, A.M. Matsumoto, T.M. Penning, S.P. Balk, E. Corey, P.S. Nelson
Administrative, technical, or material support (i.e., reporting or organizing data, constructing databases): E.A. Mostaghel, S. Hernandez, E. Corey, L.D. True, P.S. Nelson
Study supervision: E.A. Mostaghel, P.S. Nelson
Other (pathology review): M. Tretiakova

Acknowledgments

The authors wish to acknowledge reagents and technical assistance in pyrosequencing provided by Dr. William Grady, and expert technical assistance with image analysis provided by Jonathan Henriksen and NWBioSpecimen (a core service for procurement and annotation of research biospecimens), which is supported by National Cancer Institute grant P30 CA015704 (G. Gilliland, principal investigator [PI]), Institute of Translational Health Sciences grant UL1 TR000423 (M. Disis, PI), the University of Washington School of Medicine and Department of Pathology, and Fred Hutchinson Cancer Research Center, NIH Pacific Northwest Prostate Cancer SPORE P50 CA97186 (EAM, EC, LDT, PSN), NIH P01 CA163227 (EAM, TMP, SPB, EC, LDT, PSN), DOD W81XWH-12-1-0208 (EAM), NIH P30 CA015704 (JH), NIH UL1 TR000423 (JH), and Department of Veterans Affairs Puget Sound Health Care System (EAM, AMM).

The costs of publication of this article were defrayed in part by the payment of page charges. This article must therefore be hereby marked *advertisement* in accordance with 18 U.S.C. Section 1734 solely to indicate this fact.

Received May 9, 2018; revised August 1, 2018; accepted August 29, 2018; published first September 4, 2018.

References

1. Scher HI. Current management of hormone-refractory prostate cancer. Clin Adv Hematol Oncol 2004;2:724–6.
2. Stanbrough M, Bubley GJ, Ross K, Golub TR, Rubin MA, Penning TM, et al. Increased expression of genes converting adrenal androgens to testosterone in androgen-independent prostate cancer. Cancer Res 2006;66:2815–25.
3. Montgomery RB, Mostaghel EA, Vessella R, Hess DL, Kalhorn TF, Higano CS, et al. Maintenance of intratumoral androgens in metastatic prostate cancer: a mechanism for castration-resistant tumor growth. Cancer Res 2008;68:4447–54.
4. Taplin ME, Montgomery B, Logothetis CJ, Bubley GJ, Richie JP, Dalkin BL, et al. Intense androgen-deprivation therapy with abiraterone acetate plus leuprolide acetate in patients with localized high-risk prostate cancer: results of a randomized phase II neoadjuvant study. J Clin Oncol 2014;32:3705–15.
5. Arai S, Miyashiro Y, Shibata Y, Tomaru Y, Kobayashi M, Honma S, et al. Effect of castration monotherapy on the levels of adrenal androgens in cancerous prostatic tissues. Steroids 2011;76:301–8.
6. Tamae D, Mostaghel E, Montgomery B, Nelson PS, Balk SP, Kantoff PW, et al. The DHEA-sulfate depot following P450c17 inhibition supports the case for AKR1C3 inhibition in high risk localized and advanced castration resistant prostate cancer. Chemico-Biol Interact 2015;234:332–8.
7. Bhanalaph T, Varkarakis MJ, Murphy GP. Current status of bilateral adrenalectomy or advanced prostatic carcinoma. Ann Surg 1974;179:17–23.
8. Fizazi K, Tran N, Fein L, Matsubara N, Rodriguez-Antolin A, Alekseev BY, et al. Abiraterone plus prednisone in metastatic, castration-sensitive prostate cancer. N Engl J Med 2017;377:352–60.
9. Mostaghel EA. Abiraterone in the treatment of metastatic castration-resistant prostate cancer. Cancer Manag Res 2014;6:39–51.
10. Cho E, Mostaghel EA, Russell KJ, Liao JJ, Konodi MA, Kurland BF, et al. External beam radiation therapy and abiraterone in men with localized prostate cancer: safety and effect on tissue androgens. Int J Radiat Oncol Biol Phys 2015;92:236–43.
11. Mostaghel EA, Cho E, Zhang A, Alyamani M, Kaipainen A, Green S, et al. Association of tissue abiraterone levels and SLCO genotype with intraprostatic steroids and pathologic response in men with high-risk localized prostate cancer. Clin Cancer Res 2017;23:4592–601.
12. Li Z, Bishop AC, Alyamani M, Garcia JA, Dreicer R, Bunch D, et al. Conversion of abiraterone to D4A drives anti-tumour activity in prostate cancer. Nature 2015;523:347–51.
13. van Weerden WM, Bierings HG, van Steenbrugge GJ, de Jong FH, Schroder FH. Adrenal glands of mouse and rat do not synthesize androgens. Life Sci 1992;50:857–61.
14. Belanger B, Belanger A, Labrie F, Dupont A, Cusan L, Monfette G. Comparison of residual C-19 steroids in plasma and prostatic tissue of human, rat and guinea pig after castration: unique importance of extratesticular androgens in men. J Steroid Biochem 1989;32:695–8.
15. Perkins LM, Payne AH. Quantification of P450scc, P450(17) α, and iron sulfur protein reductase in Leydig cells and adrenals of inbred strains of mice. Endocrinology 1988;123:2675–82.
16. Le Goascogne C, Sananes N, Gouezou M, Takemori S, Kominami S, Baulieu EE, et al. Immunoreactive cytochrome P-450(17α) in rat and guinea-pig gonads, adrenal glands and brain. J Reprod Fertil 1991;93:609–22.
17. Pelletier G, Li S, Luu-The V, Tremblay Y, Belanger A, Labrie F. Immunoelectron microscopic localization of three key steroidogenic enzymes (cytochrome P450(scc), 3β-hydroxysteroid dehydrogenase and cytochrome P450(c17)) in rat adrenal cortex and gonads. J Endocrinol 2001;171:373–83.
18. Mostaghel EA, Marck BT, Plymate SR, Vessella RL, Balk S, Matsumoto AM, et al. Resistance to CYP17A1 inhibition with abiraterone in castration-resistant prostate cancer: induction of steroidogenesis and androgen receptor splice variants. Clin Cancer Res 2011;17:5913–25.

19. Chen J, Liang Q, Hua H, Wang Y, Luo G, Hu M, et al. Simultaneous determination of 15 steroids in rat blood via gas chromatography-mass spectrometry to evaluate the impact of emasculation on adrenal. Talanta 2009;80:826–32.
20. Ando S, Canonaco M, Beraldi E, Valenti A, Maggiolini M, Piro A, et al. The evaluation of androgen circulating levels following castration in adult male rats. Exp Clin Endocrinol 1988;91:311–8.
21. Nguyen HM, Vessella RL, Morrissey C, Brown LG, Coleman IM, Higano CS, et al. LuCaP prostate cancer patient-derived xenografts reflect the molecular heterogeneity of advanced disease and serve as models for evaluating cancer therapeutics. Prostate 2017;77:654–71.
22. Kyprianou N, Isaacs JT. Biological significance of measurable androgen levels in the rat ventral prostate following castration. Prostate 1987; 10:313–24.
23. Hu M, Xin D, Chen J, Sun G, Wang Y, Na Y. Changes in the androgen levels in the ventral prostate of spontaneously hypertensive rats after castration. BJU Int 2009;104:406–11.
24. Mongrain V, Hernandez SA, Pradervand S, Dorsaz S, Curie T, Hagiwara G, et al. Separating the contribution of glucocorticoids and wakefulness to the molecular and electrophysiological correlates of sleep homeostasis. Sleep 2010;33:1147–57.
25. Roudier MP, True LD, Higano CS, Vesselle H, Ellis W, Lange P, et al. Phenotypic heterogeneity of end-stage prostate carcinoma metastatic to bone. Hum Pathol 2003;34:646–53.
26. Roudier MP, Winters BR, Coleman I, Lam HM, Zhang X, Coleman R, et al. Characterizing the molecular features of ERG-positive tumors in primary and castration resistant prostate cancer. Prostate 2016;76: 810–22.
27. Tamae D, Byrns M, Marck B, Mostaghel EA, Nelson PS, Lange P, et al. Development, validation and application of a stable isotope dilution liquid chromatography electrospray ionization/selected reaction monitoring/mass spectrometry (SID-LC/ESI/SRM/MS) method for quantification of keto-androgens in human serum. J Steroid Biochem Mol Biol 2013; 138:281–9.
28. Rizzardi AE, Johnson AT, Vogel RI, Pambuccian SE, Henriksen J, Skubitz AP, et al. Quantitative comparison of immunohistochemical staining measured by digital image analysis versus pathologist visual scoring. Diagnostic pathology 2012;7:42.
29. Missaghian E, Kempna P, Dick B, Hirsch A, Alikhani-Koupaei R, Jegou B, et al. Role of DNA methylation in the tissue-specific expression of the CYP17A1 gene for steroidogenesis in rodents. J Endocrinol 2009;202: 99–109.
30. Hornsby PJ, Cheng CY, Lala DS, Maghsoudlou SS, Raju SG, Yang L. Changes in gene expression during senescence of adrenocortical cells in culture. J Steroid Biochem Mol Biol 1992;43:951–60.
31. Kosir R, Zmrzljak UP, Bele T, Acimovic J, Perse M, Majdic G, et al. Circadian expression of steroidogenic cytochromes P450 in the mouse adrenal gland–involvement of cAMP-responsive element modulator in epigenetic regulation of Cyp17a1. FEBS J 2012;279:1584–93.
32. Parker L, Lai M, Wolk F, Lifrak E, Kim S, Epstein L, et al. Orchiectomy does not selectively increase adrenal androgen concentrations. J Clin Endocrinol Metab 1984;59:547–50.
33. Johnsen IK, Slawik M, Shapiro I, Hartmann MF, Wudy SA, Looyenga BD, et al. Gonadectomy in mice of the inbred strain CE/J induces proliferation of sub-capsular adrenal cells expressing gonadal marker genes. J Endocrinol 2006;190:47–57.
34. Vianello S, Waterman MR, Dalla Valle L, Colombo L. Developmentally regulated expression and activity of 17α-hydroxylase/C-17,20-lyase cytochrome P450 in rat liver. Endocrinology 1997;138:3166–74.
35. Dalla Valle L, Vianello S, Belvedere P, Colombo L. Rat cytochrome P450c17 gene transcription is initiated at different start sites in extraglandular and glandular tissues. J Steroid Biochem Mol Biol 2002; 82:377–84.
36. Lam HM, McMullin R, Nguyen HM, Coleman I, Gormley M, Gulati R, et al. Characterization of an abiraterone ultraresponsive phenotype in castration-resistant prostate cancer patient-derived xenografts. Clin Cancer Res 2017;23:2301–12.
37. Li R, Evaul K, Sharma KK, Chang KH, Yoshimoto J, Liu J, et al. Abiraterone inhibits 3β-hydroxysteroid dehydrogenase: a rationale for increasing drug exposure in castration-resistant prostate cancer. Clin Cancer Res 2012; 18:3571–9.
38. Luo J, Attard G, Balk SP, Bevan C, Burnstein K, Cato L, et al. Role of androgen receptor variants in prostate cancer: report from the 2017 mission androgen receptor variants meeting. Eur Urol 2018;73:715–23.
39. Storbeck KH, Swart AC, Fox CL, Swart P. Cytochrome b5 modulates multiple reactions in steroidogenesis by diverse mechanisms. J Steroid Biochem Mol Biol 2015;151:66–73.
40. Mostaghel EA. Steroid hormone synthetic pathways in prostate cancer. Translational andrology and urology 2013;2:212–27.
41. Zhang X, Morrissey C, Sun S, Ketchandji M, Nelson PS, True LD, et al. Androgen receptor variants occur frequently in castration resistant prostate cancer metastases. PLoS ONE 2011;6:e27970.
42. Kim W, Zhang L, Wilton JH, Fetterly G, Mohler JL, Weinberg V, et al. Sequential use of the androgen synthesis inhibitors ketoconazole and abiraterone acetate in castration-resistant prostate cancer and the predictive value of circulating androgens. Clin Cancer Res 2014;20:6269–76.
43. Ryan CJ, Molina A, Li J, Kheoh T, Small EJ, Haqq CM, et al. Serum androgens as prognostic biomarkers in castration-resistant prostate cancer: results from an analysis of a randomized phase III trial. J Clin Oncol 2013;31:2791–8.
44. Ryan CJ, Peng W, Kheoh T, Welkowsky E, Haqq CM, Chandler DW, et al. Androgen dynamics and serum PSA in patients treated with abiraterone acetate. Prostate cancer and prostatic diseases 2014;17:192–8.
45. Pignatelli D, Xiao F, Gouveia AM, Ferreira JG, Vinson GP. Adrenarche in the rat. The Journal of endocrinology 2006;191:301–8.
46. Quinn TA, Ratnayake U, Dickinson H, Nguyen TH, McIntosh M, Castillo-Melendez M, et al. Ontogeny of the adrenal gland in the spiny mouse, with particular reference to production of the steroids cortisol and dehydroepiandrosterone. Endocrinology 2013;154:1190–201.
47. Bell JB, Gould RP, Hyatt PJ, Tait JF, Tait SA. Properties of rat adrenal zona reticularis cells: production and stimulation of certain steroids. J Endocrinol 1979;83:435–47.
48. Canonaco M, Ando S, Valenti A, Tavolaro R, Panno ML, Maggiolini M, et al. The in-vitro transformation of [3H]dehydroepiandrosterone into its principal metabolites in the adrenal cortex of adult castrated male rats and following steroid treatment. J Endocrinol 1989;121:419–24.
49. Ando S, Canonaco M, Valenti A, Aquila S, Tavolaro R, Maggiolini M, et al. The in vitro conversion of 3H androstenedione to testosterone and dihydrotestosterone in the adrenal gland of castrated male rat: influence of gonadal steroid administration. Exp Clin Endocrinol 1989;93:83–9.
50. Coyotupa J, Parlow AF, Kovacic N. Serum testosterone and dihydrotestosterone levels following orchiectomy in the adult rat. Endocrinology 1973;92:1579–81.
51. Kashiwagi B, Shibata Y, Ono Y, Suzuki R, Honma S, Suzuki K. Changes in testosterone and dihydrotestosterone levels in male rat accessory sex organs, serum, and seminal fluid after castration: establishment of a new highly sensitive simultaneous androgen measurement method. J Androl 2005;26:586–91.
52. Ando S, Aquila S, Beraldi E, Canonaco M, Panno ML, Valenti A, et al. Physiological changes in androgen plasma levels with elapsing of time from castration in adult male rats. Horm Metab Res 1988;20:96–9.
53. Basham KJ, Hung HA, Lerario AM, Hammer GD. Mouse models of adrenocortical tumors. Mol Cell Endocrinol 2016;421:82–97.
54. Nilsson ME, Vandenput L, Tivesten A, Norlen AK, Lagerquist MK, Windahl SH, et al. Measurement of a Comprehensive Sex Steroid Profile in Rodent Serum by High-Sensitive Gas Chromatography-Tandem Mass Spectrometry. Endocrinology 2015;156:2492–502.
55. Li Z, Alyamani M, Li J, Rogacki K, Abazeed M, Upadhyay SK, et al. Redirecting abiraterone metabolism to fine-tune prostate cancer antiandrogen therapy. Nature 2016;533:547–51.
56. Hu R, Lu C, Mostaghel EA, Yegnasubramanian S, Gurel M, Tannahill C, et al. Distinct transcriptional programs mediated by the ligand-dependent full-length androgen receptor and its splice variants in castration-resistant prostate cancer. Cancer Res 2012;72:3457–62.
57. Hu R, Dunn TA, Wei S, Isharwal S, Veltri RW, Humphreys E, et al. Ligand-independent androgen receptor variants derived from splicing of cryptic exons signify hormone-refractory prostate cancer. Cancer Res 2009;69:16–22.
58. Chen EJ, Sowalsky AG, Gao S, Cai C, Voznesensky O, Schaefer R, et al. Abiraterone treatment in castration-resistant prostate cancer selects for progesterone responsive mutant androgen receptors. Clin Cancer Res 2015;21:1273–80.

59. Kumagai J, Hofland J, Erkens-Schulze S, Dits NF, Steenbergen J, Jenster G, et al. Intratumoral conversion of adrenal androgen precursors drives androgen receptor-activated cell growth in prostate cancer more potently than de novo steroidogenesis. Prostate 2013;73: 1636–50.
60. Ando T, Nishiyama T, Takizawa I, Miyashiro Y, Hara N, Tomita Y. A carbon 21 steroidal metabolite from progestin, 20β-hydroxy-5α-dihydroprogesterone, stimulates the androgen receptor in prostate cancer cells. Prostate 2018;78:222–32.
61. Holzbeierlein J, Lal P, LaTulippe E, Smith A, Satagopan J, Zhang L, et al. Gene expression analysis of human prostate carcinoma during hormonal therapy identifies androgen-responsive genes and mechanisms of therapy resistance. Am J Pathol 2004;164:217–27.
62. Mitsiades N, Sung CC, Schultz N, Danila DC, He B, Eedunuri VK, et al. Distinct patterns of dysregulated expression of enzymes involved in androgen synthesis and metabolism in metastatic prostate cancer tumors. Cancer Res 2012;72:6142–52.
63. Hofland J, van Weerden WM, Dits NF, Steenbergen J, van Leenders GJ, Jenster G, et al. Evidence of limited contributions for intratumoral steroidogenesis in prostate cancer. Cancer Res 2010;70: 1256–64.
64. Jernberg E, Thysell E, Bovinder Ylitalo E, Rudolfsson S, Crnalic S, Widmark A, et al. Characterization of prostate cancer bone metastases according to expression levels of steroidogenic enzymes and androgen receptor splice variants. PLoS ONE 2013;8:e77407.
65. Sakai M, Martinez-Arguelles DB, Aprikian AG, Magliocco AM, Papadopoulos V. De novo steroid biosynthesis in human prostate cell lines and biopsies. The Prostate 2016;76:575–87.
66. Efstathiou E, Titus M, Tsavachidou D, Tzelepi V, Wen S, Hoang A, et al. Effects of abiraterone acetate on androgen signaling in castrate-resistant prostate cancer in bone. J Clin Oncol 2012;30:637–43.
67. Hagberg Thulin M, Nilsson ME, Thulin P, Ceraline J, Ohlsson C, Damber JE, et al. Osteoblasts promote castration-resistant prostate cancer by altering intratumoral steroidogenesis. Mol Cell Endocrinol 2016;422: 182–91.
68. Michiel Sedelaar JP, Dalrymple SS, Isaacs JT. Of mice and men–warning: intact versus castrated adult male mice as xenograft hosts are equivalent to hypogonadal versus abiraterone treated aging human males, respectively. Prostate 2013;73:1316–25.
69. Oksala R. CYP11A1 inhibition as a therapeutic approach for the treatment of castration resistant prostate cancer. J Clin Oncol 2018; 36(6_suppl):340.